Radiation Belts of Jupiter

Abstract. *Pioneer 10 counted relativistic electrons throughout the magnetosphere of Jupiter, with the greatest fluxes being inside 20 Jupiter radii. The peak flux of electrons with energy greater than 50 million electron volts was 1.3 × 10^7 per square centimeter per second at the innermost penetration of the radiation belts.*

Charged particle instruments aboard the National Aeronautics and Space Administration's Pioneer 10 spacecraft made the first in situ measurements ever of the Van Allen radiation belts of Jupiter during a 2-week passage through Jupiter's magnetosphere in early December 1973. Jupiter is the only planet besides the earth known to have a radiation belt, and the new measurements show that many features of it are in unexpected contrast to those at the earth. The onboard trapped radiation detector of the University of California, San Diego (UCSD), identified electrons with energies from 100 kev to 50 Mev and protons with energies greater than 70 Mev and measured fluxes, energy spectra, and angular distributions through the flyby.

Two different trapping regions emerge from the data. The outer region has been dubbed the magnetodisk and extends from about 20 Jupiter radii (R_J) outward. Energetic electrons are concentrated in a disk close to the tilted magnetic equator and wobble up and down past the spacecraft at the planetary rotation rate, modulating the observed flux. In addition, the electrons exhibit rapid time variations and erratic directionality with little radial dependence in flux or energy. The intensities are abruptly lower outside the magnetopause, but a trickle of relativistic electrons extend outside the bow shock (*1*, *2*) to 120 R_J. These and other particles in the magnetodisk are most easily interpreted as particles escaping outward, either torn out of the inner region by violent plasma storms or accelerated in the magnetodisk by electric potentials such as those associated with the rapid planetary rotation. This region is aptly compared with the earth's magnetic tail.

Inside 20 R_J the radiation belts assume a more ordered character, whose most dramatic feature is a steep radial intensity gradient [$\exp(-R/1.2\ R_J)$ for electrons with energy greater than 50 Mev] giving an increase in intensity of three or four orders of magnitude in all detectors. The electron energy spectrum also becomes harder closer in, the relativistic component increasing most dramatically, and the nonrelativistic component peaking and actually decreasing below 10 R_J. Just outside the magnetic shell of Europa, fluxes of electrons were $j = 3 \times 10^7$ cm^{-2} sec^{-1} ster^{-1} with energy above 0.1 Mev, and $J_0 = 1.2 \times 10^4$ cm^{-2} sec^{-1} with energy above 40 Mev. At 3.2 R_J the flux of electrons above 50 Mev was 1.3×10^7 cm^{-2} sec^{-1}, but electrons between 0.1 and 2 Mev were less than 2×10^7 cm^{-2} sec^{-1} ster^{-1}.

The spatial distribution of omnidirectional electrons with energy greater than 50 Mev is shown in Fig. 1. The counter is a small solid state detector buried in a thick omnidirectional shield. The effective area rises from 4×10^{-3} cm^2 at 27 Mev to 4×10^{-2} cm^2 above 70 Mev. Because the efficiency varies with energy, so does the conversion from count rate to flux. The fluxes in Fig. 1 were obtained by multiplying count rate by 30 cm^{-2}, but the characteristic electron energy, and thus the flux conversion factor, varies somewhat because of the hardening electron spectrum. The spacecraft trajectory, projected onto the magnetic meridian plane, is shown by the dashed line. The location where the count rate equals each contour value is marked by a circle, and each circle is reflected by symmetry through the equator. Whereas a poor magnetic field model would result in misalignment of primary and reflected circles, the present model is seen to be satisfactory out to 10 R_J.

Figure 2 shows count rates in the inner region for four data channels. Channels C2 and M1 represent rela-

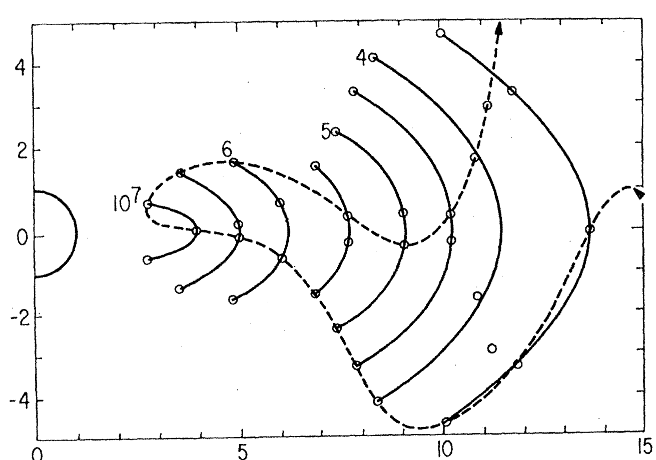

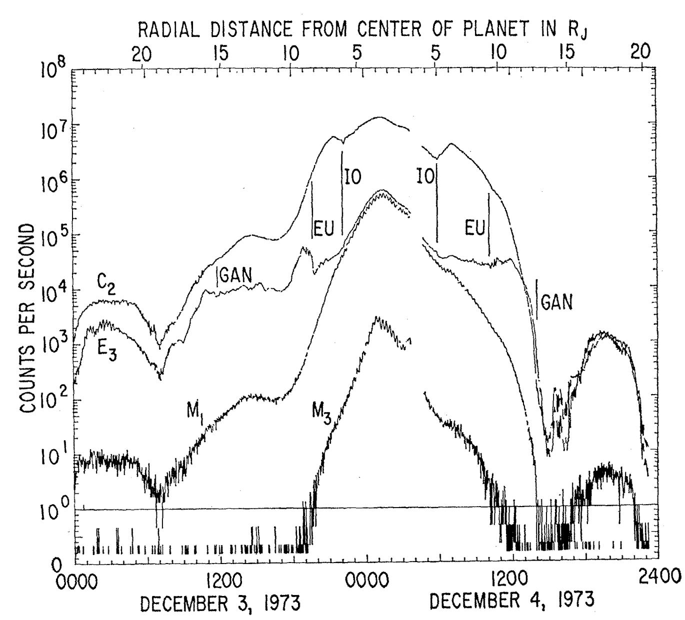

Fig. 1 (left). Contours of constant omnidirectional flux for electrons with energy greater than 50 Mev in data channel M1 (electrons per square centimeter per second). The figure represents a magnetic meridian plane according to the preliminary magnetic field model of Smith *et al.* (*2*). Fig. 2 (right). Count rates from four data channels of the UCSD trapped radiation detector. Channels C2 and M1 count relativistic electrons, E3 counts relativistic and nonrelativistic electrons, and M3 counts protons with a background of electrons. Abbreviations: *Gan*, Ganymede; *Eu*, Europa.

tivistic electrons with energy > 20 Mev and > 50 Mev. Channel E3 is the rate from a solid state detector identical to M1 except that a bent aperture in the shield permits direct access of particles that scatter by 45°. Thus E3 is susceptible to the same penetrating electrons that trigger M1 plus nonpenetrating electrons that scatter through the aperture and trigger the 0.4-Mev discriminator. Comparing E3 with C2 and M1 demonstrates the hardening of the electron spectrum toward periapsis, and differencing E3 with M1 demonstrates the loss of the nonpenetrating component below 10 R_J.

Several of the Galilean satellites are immersed in the radiation belts, and there is clear evidence that at least two of them, Io and Europa, influence the trapped particle fluxes. Marks are shown on Fig. 2 where the spacecraft crossed the dipole model magnetic shells containing Io, Europa, and Ganymede. There are prominent dips in the 20-Mev electrons at the Io shell and small fluctuations in the 0.4-Mev electrons. On the other hand, at Europa there are prominent variations in the 0.4-Mev electrons and only small effects in the 20-Mev electrons. An effect at Ganymede is questionable.

Channel M3 is a high energy discriminator on the omnidirectionally shielded solid state detector. Set high enough to have low ($< 2 \times 10^{-3}$) efficiency for electrons, this discriminator is efficient for protons between 70 and 150 Mev. The M3 response seen in Fig. 2 is caused partly by single electrons at low efficiency, partly by double coincidence of electrons, and partly by protons. When the appropriate linear and quadratic terms in M1 that represent electron background are subtracted from M3, one is left with two proton peaks, one at 0100, one at 0300, with a relative minimum between them. The second peak is clearly visible in the figure. These peaks are at the inbound and outbound crossings of the $L = 3.6$ shell, and the maximum proton intensity is $J_0 = 2.5 \times 10^4$ cm^{-2} sec^{-1}. These peaks represent the only proton fluxes visible to our counters during the flyby.

Particle identification features in the instrument design were successful in separating electrons from protons, and we name the particle species with confidence. Specifically, one of our detectors was a Cerenkov counter sensitive only to particles with velocity greater than $0.75c$ (for example, C2 in Fig. 2). There is evidence against significant proton fluxes above this energy (450 Mev) and so the counts are known to be electrons. Comparisons between the Cerenkov counter and channel M1 are in agreement, and because M3 found so few protons, M1 counted essentially all electrons.

Flux values and energy ranges are preliminary as we have not yet made proper integrations of the particle spectra over the detector responses. Therefore these numbers should be given an uncertainty of about 50 percent.

More serious data misinterpretation could arise from spacecraft charging. The expected average photoelectron flux is similar to the measured fluxes of energetic electrons inside 10 R_J. This means that, unless there is an unmeasured cold plasma component, the spacecraft may need to assume a large negative potential in order to maintain zero net current (*3*). Until it can be shown that Pioneer 10 was not driven to megavolt potentials, the present measurements cannot be safely assumed to correspond to the ambient Jovian particle fluxes. The relative absence of 0.1- to 2-Mev electrons is not firm evidence for spacecraft charging, as this would be expected for a relativistic Maxwellian distribution with a temperature over 5 Mev.

In conclusion, we note that the presence of very energetic electrons in the magnetodisk cannot be easily explained in terms of solar wind injection and convective acceleration. As an alternative, we would like to point out that interactions with the nonrotating solar wind may cause a differential rotation between the planet and the outer magnetodisk which in turn can lead to large electric fields parallel to the magnetic field lines. The expected sign and magnitude of these electric fields is such that photoelectrons in the Jovian atmosphere could be accelerated outward to very high energies. Presumably the angular distributions measured by the various detectors on Pioneer 10 will provide clues to the true nature of the injection and acceleration processes.

R. WALKER FILLIUS
CARL E. MCILWAIN
University of California, San Diego, La Jolla 92037

References and Notes

1. J. H. Wolfe, H. R. Collard, J. D. Mihalov, D. S. Intriligator, *Science* **183**, 303 (1974).
2. E. J. Smith, L. Davis, Jr., D. E. Jones, D. S. Colburn, P. J. Coleman, P. Dyal, C. P. Sonett, *ibid.*, p. 305.
3. S. E. DeForest, *J. Geophys. Res.* **77**, 651 (1972).
4. We thank G. E. Peters, E. W. Strein, and G. W. Schmidt of the University of California, San Diego, for their help in developing the instrumentation and the data reduction programs, and we thank C. F. Hall and D. Porter of the NASA/Ames Research Center for their support. This work was supported by NASA contracts NAS 2-5602 and NAS 2-6552, and by NASA grant NGL 05-005-007.

21 December 1973

Pioneer 10 Infrared Radiometer Experiment: Preliminary Results

Abstract. *Thermal maps of Jupiter at 20 and 40 micrometers show structure closely related to the visual appearance of the planet. Peak brightness temperatures of 126° and 145°K have been measured on the South Equatorial Belt, for the 20- and 40-micrometer channels, respectively. Corresponding values for the South Tropical Zone are 120° and 138°K. No asymmetries between the illuminated sunlit and nonilluminated parts of the disk were found. A preliminary discussion of the data, in terms of simple radiative equilibrium models, is presented. The net thermal energy of the planet as a whole is twice the solar energy input.*

The Jupiter Pioneer 10 infrared radiometer experiment was designed to map the planet in two wavelength ranges. On the basis of the knowledge that the thermal opacity of the Jovian atmosphere is provided mostly by the pressure-induced dipole absorption of H_2, the range from 14 to 25 μm (20-μm channel) was selected to isolate the rotational component of the H_2 spectrum. The range from 30 to 55 μm (40-μm channel) was also chosen because it contains the translational component of the H_2 spectrum, which depends on the partial pressure of He (*1*). With the channels chosen in this fashion, the sum of the powers measured in the two channels provides a measure of the net energy output, and their ratio provides a measure of *a*, the abundance ratio of He to H_2 by number (*2*). From only two radiance